Organometallics **2007,** *26,* 4663−4672

Mn(CO)$_2$ Complexes of Cyclopentadienyl/Scorpionate Hybrid Ligands

Kerstin Kunz, Hannes Vitze, Michael Bolte, Hans-Wolfram Lerner, and Matthias Wagner*

Institut für Anorganische Chemie, J.W. Goethe-Universität Frankfurt, Max-von-Laue-Strasse 7, D-60438 Frankfurt (Main), Germany

Received May 7, 2007

Rare examples of complexes featuring a chelating cyclopentadienyl/scorpionate hybrid ligand are reported. The compounds are obtained by photolytic decarbonylation of K[(OC)$_3$Mn(C$_5$H$_4$-B(pz)(R)R′)] (**1**: R = R′ = Me; **2**: R = Me, R′ = pz; **3**: R = R′ = pz; pz = pyrazol-1-yl), which leads to the constrained-geometry complexes K[(OC)$_2$Mn(C$_5$H$_4$-B(μ-pz)(R)R′)] (**4**−**6**) in quantitative yields. In **4**−**6**, the Mn-coordinating pyrazolyl ring is tethered to the cyclopentadienyl ligand via a borate bridge. According to X-ray crystallography, the molecular frameworks of **4**−**6** are largely unstrained. The ligand scaffold is thus well adapted to the coordination requirements of the Mn(I) ion. The crystal lattices of **2**, **3**, and Li[(OC)$_3$Mn(C$_5$H$_4$-BPh$_3$)] (**7**) contain dimeric aggregates held together by K$^+$-OC σ adducts, K$^+$-pz σ adducts, and K$^+$-pz π interactions (**2**, **3**) as well as Li$^+$-OC σ adducts and Li$^+$-phenyl π interactions (**7**). In none of these cases does the π-electron cloud of the cymantrenyl substituent take part in alkali metal ion complexation.

Introduction

Cyclopentadienyl derivatives[1,2] and poly(pyrazol-1-yl)borates ("scorpionates")[3,4] are among the most important ligands in transition metal chemistry. In the field of metallocene complexes, particularly interesting perspectives were opened by the introduction of bridged cyclopentadienyl systems, which give access either to oligonuclear complexes[5,6] and polymeric materials (e.g., [−(C$_5$H$_4$)Fe(C$_5$H$_4$)-SiMe$_2$−]$_n$)[7] or to mononuclear *ansa*-compounds (e.g., Me$_2$Si(C$_5$H$_4$)$_2$ZrCl$_2$).[8,9] Bridged scorpionate ligands are known with a direct B−B bond[10−12] as well as with *meta*-phenylene, *para*-phenylene,[13−15] and 1,1′-ferrocenylene[16−21] linkers. Structural motifs accessible with these compounds range from dinuclear metallamacrocycles[15] to metal-containing polymers and ferrocene-based multiple-decker sandwich complexes.[21]

Given this rich chemistry of oligo(cyclopentadienyl) and oligo(scorpionate) systems, it is an interesting challenge to combine both functionalities within the same ligand molecule and thereby to create novel cyclopentadienyl/scorpionate hybrid ligands. Two different coordination modes can be envisaged for these kinds of donor molecules: They may either adopt a bridging position between two different metal centers M^1 and M^2 (**A**, Figure 1) or, alternatively, bind to the same metal atom M via the Cp ring and one or two of their pyrazolyl substituents (**B**, Figure 1). Type **A** compounds **A1**, **A2**, and **A3** (Figure 1) are well established in the literature.[16−18,22−24] In contrast, only few examples (**B1**, **B2**; Figure 1) of type **B** metal complexes have been described and structurally characterized up to now. These are the multiple-decker sandwich complexes **B1** (M = Li$^+$−Cs$^+$)[21] and the samarium complex **B2**, which forms in a unique rearrangement reaction upon thermolysis of the precursor compound Sm[HB(pz$^{3,5-\mathrm{Me}}$)$_3$]$_2$(Cp) at 165 °C in the solid state.[25] Recently, the free cyclopentadienyl/scorpionate hybrid ligands [(C$_5$Me$_4$H)B(pz$^{3-\mathrm{Me}}$)$_3$]$^-$ and [(9-fluorenyl)Bpz$_3$]$^-$ have been

---

* Corresponding author. Fax: +49 69 798 29260. E-mail: Matthias.Wagner@chemie.uni-frankfurt.de.

[1] Long, N. J. *Metallocenes*; Blackwell Science: London, 1998.

[2] Togni, A.; Halterman, R. L. *Metallocenes: Synthesis−Reactivity−Applications*; Wiley-VCH: New York, 2006.

[3] Trofimenko, S. *Chem. Rev.* **1993**, *93*, 943−980.

[4] Trofimenko, S., *Scorpionates−The Coordination Chemistry of Polypyrazolylborate Ligands;* Imperial College Press: London, 1999.

[5] Yu, Y.; Bond, A. D.; Leonard, P. W.; Vollhardt, K. P. C.; Whitener, G. D. *Angew. Chem., Int. Ed.* **2006**, *45*, 1794−1799.

[6] Wagner, M. *Angew. Chem., Int. Ed.* **2006**, *45*, 5916−5918.

[7] Manners, I. *Adv. Organomet. Chem.* **1995**, *37*, 131−168.

[8] Bajgur, C. S.; Tikkanen, W. R.; Petersen, J. L. *Inorg. Chem.* **1985**, *24*, 2539−2546.

[9] Brintzinger, H. H.; Fischer, D.; Mülhaupt, R.; Rieger, B.; Waymouth, R. M. *Angew. Chem., Int. Ed. Engl.* **1995**, *34*, 1143−1170.

[10] Brock, C. P.; Das, M. K.; Minton, R. P.; Niedenzu, K. *J. Am. Chem. Soc.* **1988**, *110*, 817−822.

[11] Harden, N. C.; Jeffery, J. C.; McCleverty, J. A.; Rees, L. H.; Ward, M. D. *New J. Chem.* **1998**, 661−663.

[12] Armaroli, N.; Accorsi, G.; Barigelletti, F.; Couchman, S. M.; Fleming, J. S.; Harden, N. C.; Jeffery, J. C.; Mann, K. L. V.; McCleverty, J. A.; Rees, L. H.; Starling, S. R.; Ward, M. D. *Inorg. Chem.* **1999**, *38*, 5769−5776.

[13] Bieller, S.; Zhang, F.; Bolte, M.; Bats, J. W.; Lerner, H.-W.; Wagner, M. *Organometallics* **2004**, *23*, 2107−2113.

[14] Zhang, F.; Bolte, M.; Lerner, H.-W.; Wagner, M. *Organometallics* **2004**, *23*, 5075−5080.

[15] Bieller, S.; Bolte, M.; Lerner, H.-W.; Wagner, M. *Inorg. Chem.* **2005**, *44*, 9489−9496.

[16] Jäkle, F.; Polborn, K.; Wagner, M. *Chem. Ber.* **1996**, *129*, 603−606.

[17] Fabrizi de Biani, F.; Jäkle, F.; Spiegler, M.; Wagner, M.; Zanello, P. *Inorg. Chem.* **1997**, *36*, 2103−2111.

[18] Guo, S. L.; Peters, F.; Fabrizi de Biani, F.; Bats, J. W.; Herdtweck, E.; Zanello, P.; Wagner, M. *Inorg. Chem.* **2001**, *40*, 4928−4936.

[19] Ma, K.; Scheibitz, M.; Scholz, S.; Wagner, M. *J. Organomet. Chem.* **2002**, *652*, 11−19.

[20] Haghiri Ilkhechi, A.; Bolte, M.; Lerner, H.-W.; Wagner, M. *J. Organomet. Chem.* **2005**, *690*, 1971−1977.

[21] Haghiri Ilkhechi, A.; Mercero, J. M.; Silanes, I.; Bolte, M.; Scheibitz, M.; Lerner, H.-W.; Ugalde, J. M.; Wagner, M. *J. Am. Chem. Soc.* **2005**, *127*, 10656−10666.

[22] Herdtweck, E.; Peters, F.; Scherer, W.; Wagner, M. *Polyhedron* **1998**, *17*, 1149−1157.

[23] Guo, S. L.; Bats, J. W.; Bolte, M.; Wagner, M. *J. Chem. Soc., Dalton Trans.* **2001**, 3572−3576.

[24] Haghiri Ilkhechi, A.; Guo, S. L.; Bolte, M.; Wagner, M. *Dalton Trans.* **2003**, 2303−2307.

[25] Lopes, I.; Lin, G. Y.; Domingos, A.; McDonald, R.; Marques, N.; Takats, J. *J. Am. Chem. Soc.* **1999**, *121*, 8110−8111.

10.1021/om700450j CCC: $37.00

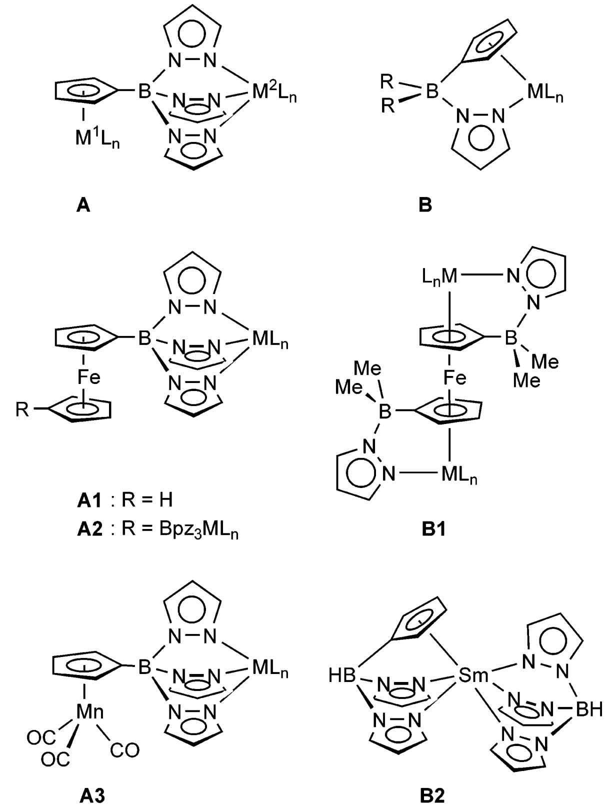

Figure 1. Bridging (**A**) and chelating (**B**) coordination mode of cyclopentadienyl/poly(pyrazol-1-yl)borate hybrid ligands; representative examples **A1**−**B2** for which these coordination modes have been realized. **B2**: CH_3 groups in the 3 and 5 positions of all pyrazolyl rings are omitted for clarity.

prepared, but their ligand properties are still largely unexplored.[26,27]

The purpose of this paper is to describe the synthesis and molecular structure of **B**-type $Mn(CO)_2$ complexes that are readily available from cymantrenylpoly(pyrazol-1-yl)borates (cf. **A3**, M = K^+) by replacement of one CO ligand with a pyrazolyl nitrogen atom.

Results and Discussion

Synthesis. The cymantrenylmono(pyrazol-1-yl)borate **1** was obtained from Kpz and $CymBMe_2$[28] via B−N adduct formation (Scheme 1; pz = pyrazolide; Cym = cymantrenyl).

The corresponding bis(pyrazol-1-yl)borate **2** (Scheme 1) readily formed upon treatment of $CymB(NMe_2)Me$ with an equimolar mixture of Kpz and Hpz. One equivalent of $HNMe_2$ is liberated in the course of the reaction.

Finally, deprotonation of the free acid $H[CymBpz_3]$[23] with KO*t*Bu gave the potassium tris(pyrazol-1-yl)borate **3** in almost quantitative yield (Scheme 1).

Irradiation of THF solutions of **1**−**3** in borosilicate glass vessels with a high-pressure mercury lamp ($\lambda_{max} = 510$ nm) led to the replacement of CO by a pyrazolyl ring and thus created the complexes **4**−**6** with chelating cyclopentadienyl/scorpionate hybrid ligands (Scheme 2). Complexes **4**−**6** also form when the precursor compounds **1**−**3** are exposed to daylight in THF over a period of several days. Under these conditions, the transformation is fastest for **1** and slowest for **3**. Single crystals of **4**(18-c-6)−**6**(18-c-6) were grown from toluene or toluene/THF solutions of **4**−**6** to which excess 18-crown-6 had been added.

Scheme 1. Synthesis of the Cymantrenylmono-, Cymantrenylbis-, and Cymantrenyltris(pyrazol-1-yl)borate Salts 1−3[a]

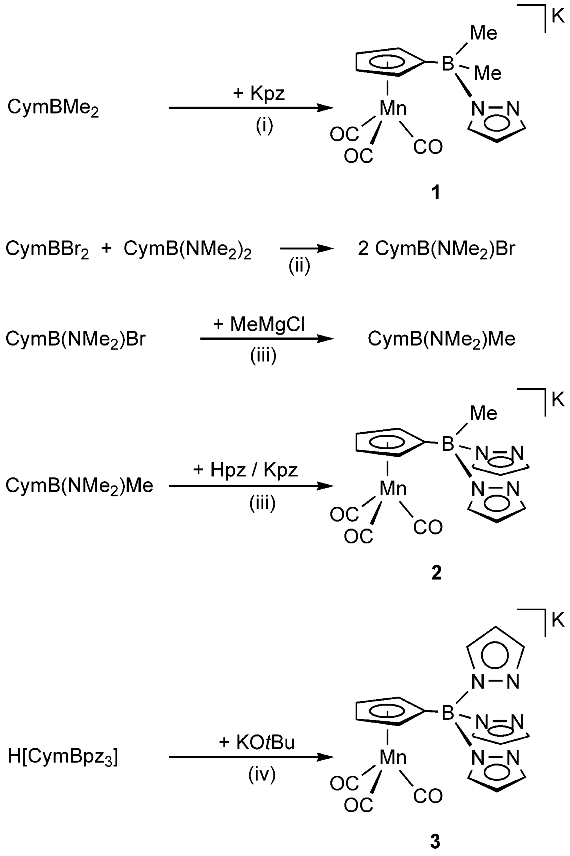

[a] Cym = cymantrenyl, pz = pyrazol-1-yl; (i) toluene/THF, −78 °C to rt; (ii) toluene, rt; (iii) toluene/THF, −78 °C to rt; (iv) THF, 0 °C.

An X-ray crystal structure analysis of the THF adduct of **3** revealed that the K^+ ions are bound to some of the pyrazolyl substituents via their nitrogen lone pair and to others via their electron π system (see below). The π faces of the cyclopentadienyl rings, however, do not contribute to K^+ coordination. This is in contrast to the behavior of the alkali metal salts of analogous ferrocenyl scorpionate ligands, which tend to establish multiple-decker sandwich structures in the solid state.[20,21,29,30] We have synthesized the lithium cymantrenylborate **7** in order to investigate whether a M^+-η^5-$(C_5H_4R)Mn(CO)_3$ arrangement can be brought about when (i) K^+ is replaced by the more strongly π coordinating Li^+ ion[21] and (ii) no Lewis basic nitrogen donor sites are present that could compete with the cyclopentadienyl ring for Li^+ binding. Compound **7** is accessible from $CymBBr_2$[28] and a solution of PhLi in dibutyl ether. $Li[BPh_4]$ was formed as a byproduct irrespective of the reaction conditions applied.

---

(26) Roitershtein, D.; Domingos, A.; Marques, N. *Organometallics* **2004**, *23*, 3483−3487. For a related bis(pyrazol-1-yl)methane ligand see: Otero, A.; Fernández-Baeza, J.; Antiñolo, A.; Tejeda, J.; Lara-Sánchez, A.; Sánchez-Barba, L.; Rodríguez, A. M.; Maestro, M. A. *J. Am Chem. Soc.* **2004**, *126*, 1330−1331.

(27) Bieller, S.; Bolte, M.; Lerner, H.-W.; Wagner, M. *J. Organomet. Chem.* **2005**, *690*, 1935−1946.

(28) Renk, T.; Ruf, W.; Siebert, W. *J. Organomet. Chem.* **1976**, *120*, 1−25.

(29) Haghiri Ilkhechi, A.; Scheibitz, M.; Bolte, M.; Lerner, H.-W.; Wagner, M. *Polyhedron* **2004**, *23*, 2597−2604.

(30) Kaufmann, L.; Vitze, H.; Bolte, M.; Lerner, H.-W.; Wagner, M. *Organometallics* **2007**, *26*, 1771−1776.

Scheme 2. Synthesis of the Mn(CO)$_2$ Complexes 4−6 with Chelating Cyclopentadienyl/Scorpionate Hybrid Ligands; Synthesis of Lithium Cymantrenyltris(phenyl)borate 7 and of the Pyrazole Complex 8[a]

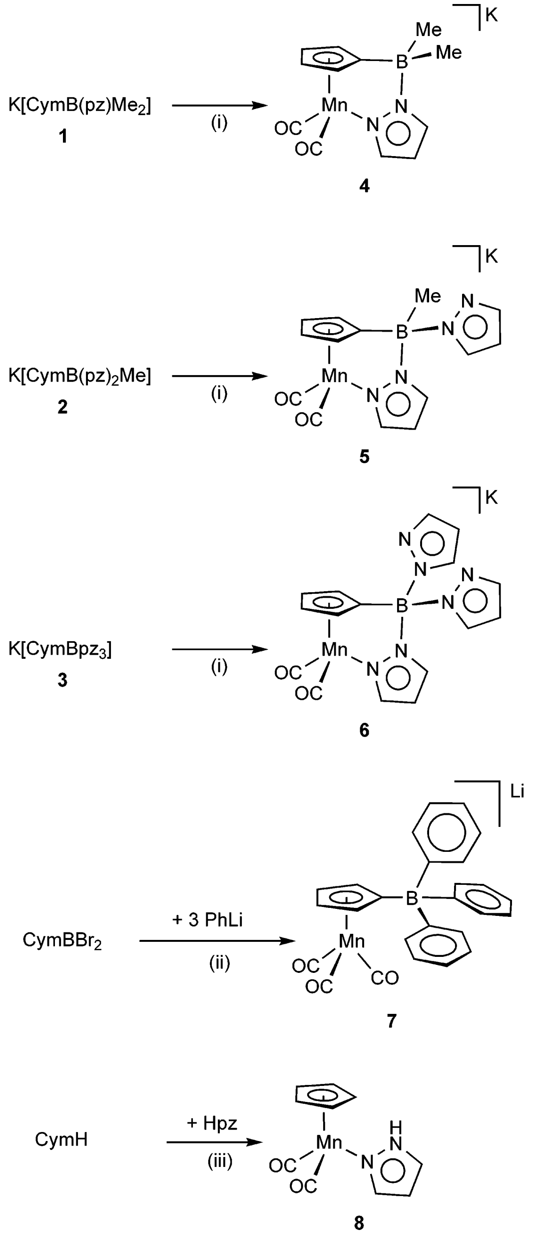

[a] (i) THF, UV irradiation; (ii) toluene/Bu$_2$O, −78 °C to rt; (iii) Et$_2$O, UV irradiation.

The pyrazole complex **8** (Scheme 2) was structurally characterized in order to be able to compare the Mn−N(pz) bond lengths of the constrained-geometry complexes **4**(18-c-6)−**6**(18-c-6) with the corresponding bond length in a closely related unbridged species. Even though irradiation of a 1:1 mixture of cymantrene and pyrazole in diethyl ether with a high-pressure mercury lamp ($\lambda_{\max} = 510$ nm; 50 h) did not lead to complete conversion, we were able to isolate a few single crystals of **8** that were suitable for X-ray crystallography.

Spectroscopic Characterization. *Note*: In the cases of the complexes **4**−**6** we are reporting the NMR data of their crown ether adducts **4**(18-c-6)−**6**(18-c-6) because here the signal resolution is least affected by cation/anion association−dissociation equilibria.

The ^{11}B NMR signals of the complexes **1**−**6**(18-c-6) appear in the interval between 0.1 and −8.7 ppm, which testifies to the presence of tetracoordinated boron atoms.[31,32] In both series **1**−**3** and **4**(18-c-6)−**6**(18-c-6), a continuous downfield shift of the ^{11}B resonance is observed upon replacement of methyl substituents for more electronegative pyrazolyl rings; there are no significant differences between the ^{11}B resonances of an open-chain species and its corresponding chelate complex [cf. $\delta(^{11}\text{B}) = -8.7$ (**1**), −1.1 (**2**), 0.1 (**3**); −8.1 (**4**(18-c-6)), −2.0 (**5**(18-c-6)), −0.1 (**6**(18-c-6))]. In line with these arguments, the tetraorganylborate **7** [$\delta(^{11}\text{B}) = -9.5$] possesses the most shielded ^{11}B nucleus of all complexes **1**−**7**.

In the ^{1}H NMR spectrum of **1**, the cymantrenyl substituent gives rise to two resonances for the α and β protons (4.45 ppm, 4.46 ppm). Moreover, three signals at 5.94, 7.24, and 7.46 ppm can be assigned to the three chemically nonequivalent protons of the pyrazolyl ring. The ^{1}H NMR spectra of **2** and **3** are characterized by similar signal patterns and chemical shift values. However, the integral ratio between the cymantrenyl and pyrazolyl resonances is no longer 4:3 as in **1**, but 4:6 (**2**) and 4:9 (**3**), in agreement with the presence of bis- and tris(pyrazol-1-yl)borate moieties. As to be expected, complex **7** shows two signals in the cyclopentadienyl range and one set of three resonances for the three chemically equivalent phenyl rings (integral ratio C$_5$H$_4$:Ph = 4:15).

Upon going from **1** to **4**(18-c-6), one of the cymantrenyl proton signals experiences an upfield shift of almost 1 ppm ($\delta(^1\text{H}) = 3.53$), whereas the second signal appears at significantly lower field ($\delta(^1\text{H}) = 4.93$). Similarly increased shift differences between the α and β proton resonances are also evident for **5**(18-c-6) and **6**(18-c-6). Most importantly, the two α protons as well as the two β protons of **5**(18-c-6) are not chemically equivalent but give rise to a total number of four resonances (integral ratio 1:1:1:1). This feature can easily be explained by the fact that the boron atom of **5**(18-c-6) becomes a chiral center once one of the two pyrazolyl substituents gets attached to the Mn(I) ion. In accordance with this interpretation, the ^{1}H NMR spectrum of **5**(18-c-6) gives clear evidence for the presence of two chemically inequivalent pyrazolyl rings (six resonances, each integrating 1H, in the chemical shift range between 5.84 and 7.31 ppm). As to be expected, the proton NMR spectrum of the more symmetrical tris(pyrazol-1-yl)borate **6**(18-c-6) is characterized by only two cymantrenyl proton resonances as well as by two sets of pyrazolyl signals with an integral ratio Cym:pz:pz* = 4:6:3.

The ^{13}C NMR spectra of **1**−**7** fully support the interpretation outlined above; signals for the *ipso*-carbon atoms of the cyclopentadienyl rings are broadened beyond detection due to quadrupolar relaxation and $^1J_{\text{CB}}$ coupling.

In the IR spectrum, parent cymantrene has CO vibrations at 2035 cm^{-1} (A$_1$) and 1949 cm^{-1} (E) compared to values $\tilde{\nu}$(CO) = 2004 cm^{-1}/1910 cm^{-1}, 2009 cm^{-1}/1920 cm^{-1}, and 2006 cm^{-1}/1921 cm^{-1} for **1**, **2**, and **3**, respectively (KBr pellets). This leads to the conclusion that a (pyrazol-1-yl)borate substituent increases the charge density on the Mn(I) ion, thereby leading to more extensive metal-to-carbonyl π back-bonding (cf. also **7**: $\tilde{\nu}$(CO) = 2000 cm^{-1}/1911 cm^{-1}). A related effect has been observed in the case of numerous different ferrocenyl derivatives [Fc-BR$_3$]$^{0/-}$, which are easier to oxidize than ferrocene itself.[20,21,33−36] In the half-sandwich chelate complexes **4**−**6**, the CO bands exhibit a further red shift and appear

---

(31) Nöth, H.; Wrackmeyer, B. Nuclear Magnetic Resonance Spectroscopy of Boron Compounds. In *NMR Basic Principles and Progress*; Diehl, P., Fluck, E., Kosfeld, R., Eds.; Springer: Berlin, 1978.

(32) Mason, J. *Multinuclear NMR*; Plenum Press: New York, 1987.

(33) Fontani, M.; Peters, F.; Scherer, W.; Wachter, W.; Wagner, M.; Zanello, P. *Eur. J. Inorg. Chem.* **1998**, 1453−1465.

Table 1. Selected Crystallographic Data for CymBBr$_2$, (2THF)$_2$, (3THF)$_2$, 4(18-c-6), 5(18-c-6), and 6(18-c-6)

	CymBBr$_2$	(**2**THF)$_2$	(**3**THF)$_2$
formula	$C_8H_4BBr_2MnO_3$	$C_{38}H_{42}B_2K_2Mn_2N_8O_8$	$C_{21}H_{21}BKMnN_6O_4$
fw	373.68	948.50	526.29
color, shape	light yellow, block	light yellow, plate	yellow, block
temp (K)	173(2)	173(2)	173(2)
radiation	Mo Kα, 0.71073 Å	Mo Kα, 0.71073 Å	Mo Kα, 0.71073 Å
cryst syst	orthorhombic	monoclinic	triclinic
space group	*Pbca*	*P*2/*c*	$P\bar{1}$
a (Å)	13.6364(13)	11.8591(11)	9.7794(11)
b (Å)	12.0796(11)	8.2372(5)	11.5583(14)
c (Å)	13.9393(11)	23.1905(19)	12.2180(16)
α (deg)	90	90	105.250(10)
β (deg)	90	100.310(7)	109.593(9)
γ (deg)	90	90	101.044(9)
V (Å^3)	2296.1(4)	2228.8(3)	1194.3(3)
Z	8	2	2
D_{calcd} (g cm^{-3})	2.162	1.413	1.463
F(000)	1408	976	540
μ (mm^{-1})	8.090	0.811	0.767
cryst size (mm^3)	0.17 × 0.15 × 0.09	0.31 × 0.27 × 0.13	0.51 × 0.48 × 0.35
no. of rflns collected	15 920	11 899	9394
no. of indep rflns (R_{int})	2159 (0.0915)	4147 (0.0394)	4382 (0.0493)
no. of data/restraints/params	2159/0/136	4147/20/292	4382/0/327
GOOF on F^2	1.084	1.024	1.049
R1, wR2 ($I > 2\sigma(I)$)	0.0618, 0.1048	0.0373, 0.0951	0.0493, 0.1330
R1, wR2 (all data)	0.0979, 0.1148	0.0491, 0.0997	0.0550, 0.1370
largest diff peak and hole (e Å^{-3})	0.609, −0.706	0.631, −0.290	0.743, −1.192

	4(18-c-6)	**5**(18-c-6)	**6**(18-c-6)
formula	$C_{24}H_{37}BKMnN_2O_8$	$C_{26}H_{37}BKMnN_4O_8 \times C_7H_8$	$C_{28}H_{37}BKMnN_6O_8$
fw	586.41	730.58	690.49
color, shape	red, block	orange, needle	orange, plate
temp (K)	173(2)	173(2)	173(2)
radiation	Mo Kα, 0.71073 Å	Mo Kα, 0.71073 Å	Mo Kα, 0.71073 Å
cryst syst	triclinic	triclinic	monoclinic
space group	$P\bar{1}$	$P\bar{1}$	$P2_1/n$
a (Å)	10.8194(7)	10.3349(7)	13.0269(7)
b (Å)	11.6661(7)	10.4943(7)	16.1183(9)
c (Å)	13.3634(9)	18.0340(12)	15.9486(10)
α (deg)	115.469(5)	82.379(6)	90
β (deg)	91.690(5)	76.520(5)	96.974(5)
γ (deg)	106.515(5)	76.384(5)	90
V (Å^3)	1437.38(16)	1842.3(2)	3324.0(3)
Z	2	2	4
D_{calcd} (g cm^{-3})	1.355	1.317	1.380
F(000)	616	768	1440
μ (mm^{-1})	0.650	0.524	0.578
cryst size (mm^3)	0.50 × 0.40 × 0.20	0.54 × 0.10 × 0.09	0.27 × 0.24 × 0.12
no. of rflns collected	24 723	27 445	30 917
no. of indep rflns (R_{int})	5369 (0.0460)	7482 (0.0537)	6242 (0.0809)
no. of data/restraints/params	5369/0/335	7482/31/433	6242/0/407
GOOF on F^2	1.038	1.018	1.014
R1, wR2 ($I > 2\sigma(I)$)	0.0267, 0.0674	0.0470, 0.1202	0.0407, 0.0956
R1, wR2 (all data)	0.0296, 0.0689	0.0608, 0.1274	0.0620, 0.1021
largest diff peak and hole (e Å^{-3})	0.257, −0.292	1.146, −0.543	0.780, −0.362

at $\tilde{\nu}$(CO) = 1891 cm^{-1}/1817 cm^{-1}, 1890 cm^{-1}/1813 cm^{-1}, and 1902 cm^{-1}/1824 cm^{-1}, respectively (KBr pellets). These values are considerably lower than those measured for the neutral complex dicarbonyl[η^5-(8-quinolyl)cyclopentadienyl]manganese(I) ($\tilde{\nu}$(CO) = 1928 cm^{-1}/1864 cm^{-1}; toluene solution)[37] but agree well with the CO stretching frequencies reported for several (C_5H_4R)Mn(CO)$_2$ complexes featuring chelating (pyrazol-1-yl)methyl sidearms R.[38−42] The neutral pyrazole complex **8** is characterized by $\tilde{\nu}$(CO) values of 1913 and 1837 cm^{-1}.

In the electronic spectrum, cymantrene has a well-defined ultraviolet transition maximizing near 330 nm (ϵ = 1100 L·mol^{-1}·cm^{-1}).[43] The corresponding absorption maximum of the tris(pyrazol-1-yl)borate **3** is also observed at λ_{max} = 330 nm (ϵ = 1110 L·mol^{-1}·cm^{-1}). The UV/vis spectrum of the complex **6** is characterized by two bands in the UV region (λ_{max} = 280 nm (ϵ = 2990 L·mol^{-1}·cm^{-1}), 312 nm (ϵ = 2770 L·mol^{-1}·cm^{-1})) and an additional extremely broad absorption with an onset at about 550 nm (ϵ(400 nm) = 390 L·mol^{-1}·cm^{-1}).

---

(34) Scheibitz, M.; Winter, R. F.; Bolte, M.; Lerner, H.-W.; Wagner, M. *Angew. Chem., Int. Ed.* **2003**, *42*, 924−927.

(35) Scheibitz, M.; Bolte, M.; Bats, J. W.; Lerner, H.-W.; Nowik, I.; Herber, R. H.; Krapp, A.; Lein, M.; Holthausen, M. C.; Wagner, M. *Chem.−Eur. J.* **2005**, *11*, 584−603.

(36) Scheibitz, M.; Heilmann, J. B.; Winter, R. F.; Bolte, M.; Bats, J. W.; Wagner, M. *Dalton Trans.* **2005**, 159−170.

(37) Enders, M.; Kohl, G.; Pritzkow, H. *J. Organomet. Chem.* **2001**, *622*, 66−73.

(38) Röder, J. C.; Meyer, F.; Kaifer, E. *Angew. Chem., Int. Ed.* **2002**, *41*, 2304−2306.

(39) Röder, J. C.; Meyer, F.; Winter, R. F.; Kaifer, E. *J. Organomet. Chem.* **2002**, *641*, 113−120.

(40) Röder, J. C.; Meyer, F.; Hyla-Kryspin, I.; Winter, R. F.; Kaifer, E. *Chem.−Eur. J.* **2003**, *9*, 2636−2648.

(41) Sheng, T.; Dechert, S.; Hyla-Kryspin, I.; Winter, R. F.; Meyer, F. *Inorg. Chem.* **2005**, *44*, 3863−3874.

(42) Sheng, T.; Dechert, S.; Stückl, A. C.; Meyer, F. *Eur. J. Inorg. Chem.* **2005**, 1293−1302.

Table 2. Selected Crystallographic Data for (7OBu$_2$)$_2$ and 8

	(**7**OBu$_2$)$_2$	**8**
formula	$C_{34}H_{37}BLiMnO_4$	$C_{10}H_9MnN_2O_2$
fw	582.33	244.13
color, shape	light yellow, plate	orange, block
temp (K)	173(2)	173(2)
radiation	Mo Kα, 0.71073 Å	Mo Kα, 0.71073 Å
cryst syst	triclinic	monoclinic
space group	$P\bar{1}$	$P2_1/n$
a (Å)	10.8317(13)	7.8006(10)
b (Å)	13.0141(16)	9.3963(8)
c (Å)	13.2055(15)	14.4520(18)
α (deg)	109.377(9)	90
β (deg)	114.001(9)	90.860(10)
γ (deg)	96.173(8)	90
V (Å^3)	1539.4(3)	1059.2(2)
Z	2	4
D_{calcd} (g cm^{-3})	1.256	1.531
F(000)	612	496
μ (mm^{-1})	0.464	1.225
cryst size (mm^3)	0.28 × 0.14 × 0.04	0.23 × 0.22 × 0.18
no. of rflns collected	14 175	13 952
no. of indep rflns (R_{int})	5734 (0.0861)	1979 (0.0930)
no. of data/restraints/ params	5734/0/370	1979/0/136
GOOF on F^2	0.955	1.142
R1, wR2 ($I > 2\sigma(I)$)	0.0662, 0.1489	0.0425, 0.0934
R1, wR2 (all data)	0.1179, 0.1700	0.0499, 0.0964
largest diff peak and hole (e Å^{-3})	0.856, −0.524	0.377, −0.491

It is known that the low-energy region of the electronic absorption spectra of pyridine complexes $(C_5H_5)Mn(CO)_2py$ is dominated by a Mn(I) → π*-pyridine CT absorption.[43] We therefore tentatively assign the band at $\lambda_{max} \approx 400$ nm in the UV/vis spectrum of **6** to a Mn(I) → π*-pyrazolyl CT transition.

Electrochemical Investigation. The formal electrode potentials $E_{1/2}$ (vs FcH/FcH$^+$) for the Mn(I)/Mn(II) redox transitions of **4**(18-c-6), **5**(18-c-6), and **6**(18-c-6) are −0.82, −0.72, and −0.63 V, respectively (THF solutions, [NBu$_4$][PF$_6$] (0.1 mol·L^{-1}) as supporting electrolyte; for electrochemical data of related complexes see refs 38−42). These redox transitions are chemically reversible, as evidenced by the following criteria: the current ratios i_{pc}/i_{pa} are constantly equal to 1, the current functions $i_{pa}/v^{1/2}$ remain constant, and the peak-to-peak separations ΔE are very close to the value found for the internal ferrocene standard (ΔE = 109 mV for **4**(18-c-6), 104 mV for **5**(18-c-6), 99 mV for **6**(18-c-6); v = 0.1 V s^{-1}). We note a pronounced influence of the substituents at boron on the redox potentials of our compounds. Replacement of one methyl group by an electronegative pyrazolyl ring leads to an anodic shift of about 0.1 V.

X-ray Crystal Structure Determination. Crystal data and structure refinement details for CymBBr$_2$ and (**2**THF)$_2$−**8** are compiled in Tables 1 and 2.

Even though cymantrenyl(dihalo)boranes were first prepared more than 30 years ago,[28] their crystal structures remained unknown until very recently. This is mainly due to the fact that they are normally isolated as oily products. In 2006, Braunschweig et al. determined the solid-state structure of (methylcymantrenyl)(dibromo)borane (Cym^{Me}BBr$_2$).[44] Our group now succeeded in growing single crystals of the parent compound CymBBr$_2$ from hexane (Figure 2; Cym = cymantrenyl). As to be expected, the molecules of Cym^{Me}BBr$_2$ and CymBBr$_2$ possess very similar structures in the solid state. The most important features are the following: (i) Each boron atom is coordinated in a trigonal-planar fashion. (ii) Each BBr$_2$ group is bent out of the plane of its cyclopentadienyl ring toward the Mn(I) center by a dip angle α* of 11.4° in CymBBr$_2$ and 12.3° in Cym^{Me}BBr$_2$ (α* = 180° − α; α is the angle between the geometric center of the carbon atoms constituting the substituted cyclopentadienyl ring, the *ipso* carbon atom, and the boron atom). (iii) There is a characteristic C−C bond length alternation within the cyclopentadienyl rings, giving the $Br_2B-C_5H_4$ moieties some borafulvene character. This effect manifests itself in higher reliability in the case of Cym^{Me}BBr$_2$, for which the bond lengths have been determined with lower error margins.[44] Similar structural peculiarities as in the cymantrenyl(dibromo)boranes are evident in the cation $[(Ph_2C-C_5H_4)Mn(CO)_3]^+$, which bears an *exo* methylene group instead of the BBr$_2$ substituent and has been described as a η^5-diphenylfulvene complex (dip angle: 6.6°).[45] In spite of these remarkable similarities of the molecular frameworks, there appear to be important differences in the electronic structures of $[(Ph_2C-C_5H_4)Mn(CO)_3]^+$ and the cymantrenylboranes. For example, the tetrakis[3,5-bis(trifluoromethyl)phenyl]borate salt of $[(Ph_2C-C_5H_4)Mn(CO)_3]^+$ is a deep blue compound, whereas CymBBr$_2$ and Cym^{Me}BBr$_2$ are yellow colored.

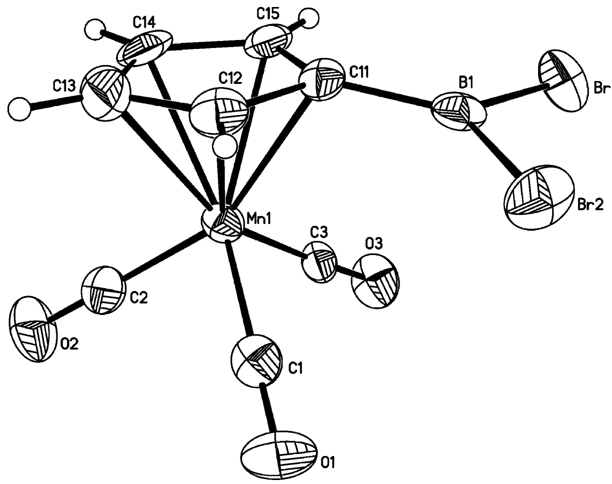

Figure 2. Structure of CymBBr$_2$ in the crystal. Thermal ellipsoids are drawn at the 50% probability level. Selected bond lengths (Å) and angles (deg): B(1)−Br(1) = 1.940(10), B(1)−Br(2) = 1.935(8), B(1)−C(11) = 1.510(12), C(11)−C(12) = 1.428(11), C(12)−C(13) = 1.422(12), C(13)−C(14) = 1.441(13), C(14)−C(15) = 1.410(13), C(11)−C(15) = 1.451(10); Br(1)−B(1)−Br(2) = 116.4(5), C(11)−B(1)−Br(1) = 122.1(5), C(11)−B(1)−Br(2) = 121.5(6), α* = 11.4.

The potassium bis(pyrazol-1-yl)borate **2** crystallizes together with 1 equivalent of THF in the form of C_2-symmetric dimers with bridging scorpionate ligands ((**2**THF)$_2$; Figure 3). Each of these two ligands binds to one potassium cation via two pyrazolyl rings and to the other via one pyrazolyl ring: The N(31)-pyrazolyl substituent acts as a σ donor toward K(1) (K(1)−N(32) = 2.826(2) Å). The N(41)-pyrazolyl ring binds to K(1) in an η^5 manner (K(1)···COG(pz) = 3.121 Å) and to K(1$^\#$) via the nitrogen lone pair (K(1$^\#$)−N(42) = 2.805(2) Å). The coordination sphere of each K$^+$ ion is completed by one THF molecule and two carbonyl oxygen atoms (*intra*dimer contact: K(1)−O(3$^\#$) = 3.133(3) Å; *inter*dimer contact: K(1)−O(2*) = 2.925(2) Å).

Single crystals of the potassium tris(pyrazol-1-yl)borate **3** were grown from THF/pentane (1:1). Similar to the potassium

---

(43) Giordano, P. J.; Wrighton, M. S. *Inorg. Chem.* **1977**, *16*, 160−166.

(44) Braunschweig, H.; Kraft, M.; Schwarz, S.; Seeler, F.; Stellwag, S. *Inorg. Chem.* **2006**, *45*, 5275−5277.

(45) Volland, M. A. O.; Kudis, S.; Helmchen, G.; Hyla-Kryspin, I.; Rominger, F.; Gleiter, R. *Organometallics* **2001**, *20*, 227−230.

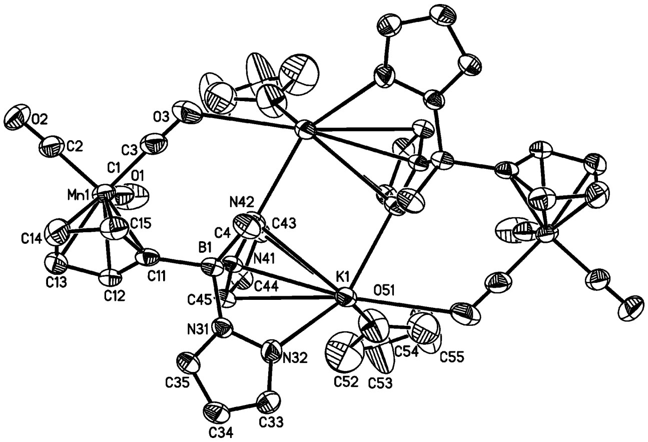

Figure 3. Structure of ($\mathbf{2}$THF)$_2$ in the crystal. Hydrogen atoms are omitted for clarity; thermal ellipsoids are drawn at the 50% probability level. Selected bond lengths (Å), atom···atom distances (Å), angles (deg), and torsion angles (deg): B(1)−C(4) = 1.618(3), B(1)−C(11) = 1.625(4), B(1)−N(31) = 1.580(3), B(1)−N(41) = 1.577(3), K(1)−N(32) = 2.826(2), K(1)−N(42) = 3.166(2), K(1$^{\#}$)−N(42) = 2.805(2), K(1)−O(3$^{\#}$) = 3.133(3), K(1)−O(2*) = 2.925(2), K(1)···COG(pz) = 3.121, K(1)···K(1$^{\#}$) = 4.460(1); N(31)−B(1)−N(41) = 104.9(2); B(1)−N(31)−N(32)−K(1) = −8.8(3), B(1)−N(41)−N(42)−K(1$^{\#}$) = 21.6(4). COG(pz): center of gravity of the N(41)-pyrazolyl ring. Symmetry transformations used to generate equivalent atoms: $-x+1$, y, $-z+3/2$ (#), $x-1$, y, z (*).

bis(pyrazol-1-yl)borate **2**, the crystal lattice of **3** consists of dimeric units (($\mathbf{3}$THF)$_2$; Figure 4). However, in contrast to ($\mathbf{2}$THF)$_2$, the two halves of each dimer of ($\mathbf{3}$THF)$_2$ are related by an inversion center rather than by a 2-fold rotation axis. Irrespective of that, the main structural motifs of both compounds are largely the same (($\mathbf{3}$THF)$_2$: K(1)−N(32) = 2.924(2) Å, K(1)···COG(pz) = 3.069 Å, K(1$^{\#}$)−N(42) = 2.738(2) Å; *intra*dimer contact K(1)−O(3$^{\#}$) = 3.009(2) Å; *inter*dimer contact K(1)−O(1*) = 2.969(2) Å). The additional N(21)-pyrazolyl ring of **3** coordinates K(1$^{\#}$) at a bond length K(1$^{\#}$)−N(22) of 2.912(2) Å with a torsion angle B(1)−N(21)−N(22)−K(1$^{\#}$) of 70.8(2)°. This indicates the K$^+$ ion to interact not only with the lone pair of N(22) but also with its p orbital. Interestingly, the structure of ($\mathbf{3}$THF)$_2$ closely resembles the structure of the dimeric ferrocenyl scorpionate {[K(THF)][FcB(Me)pz$_2$]}$_2$.[20] Here, a methyl group replaces the cymantrenyl substituent, while the C$_5$H$_4$ ring of the ferrocenyl fragment takes the place of the N(21)-pyrazolyl ring and acts as a π donor toward K(1$^{\#}$). π-Coordination of ferrocene to main-group metal ions is not an uncommon phenomenon.[21,29,30,46−52] We thus find it interesting to see that in ($\mathbf{2}$THF)$_2$ and ($\mathbf{3}$THF)$_2$ the cyclopentadienyl rings do not engage in this kind of behavior, which may be attributed to the facts that the Mn(CO)$_3$ fragment is electron-withdrawing and provides three Lewis basic carbonyl oxygen atoms as alternative donor sites.

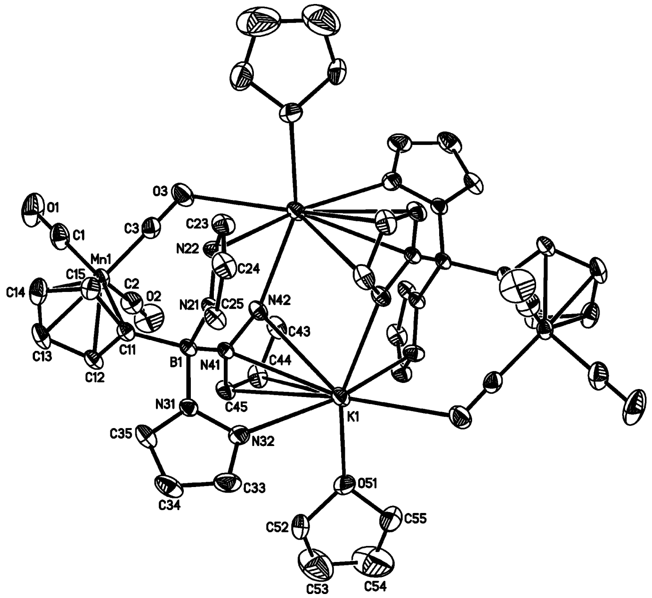

Figure 4. Structure of ($\mathbf{3}$THF)$_2$ in the crystal. Hydrogen atoms are omitted for clarity; thermal ellipsoids are drawn at the 50% probability level. Selected bond lengths (Å), atom···atom distances (Å), angles (deg), and torsion angles (deg): B(1)−C(11) = 1.623(3), B(1)−N(21) = 1.554(3), B(1)−N(31) = 1.553(3), B(1)−N(41) = 1.567(3), K(1)−N(22$^{\#}$) = 2.912(2), K(1)−N(32) = 2.924(2), K(1)−N(42) = 3.186(2), K(1)−N(42$^{\#}$) = 2.738(2), K(1)−O(3$^{\#}$) = 3.009(2), K(1)−O(1*) = 2.969(2), K(1)···COG(pz) = 3.069, K(1)···K(1$^{\#}$) = 4.749; N(21)−B(1)−N(31) = 106.6(2), N(21)−B(1)−N(41) = 113.1(2), N(31)−B(1)−N(41) = 105.7(2); B(1)−N(21)−N(22)−K(1$^{\#}$) = 70.8(2), B(1)−N(31)−N(32)−K(1) = 12.6(3), B(1)−N(41)−N(42)−K(1) = −105.9(2), B(1)−N(41)−N(42)−K(1$^{\#}$) = −7.1(4). COG(pz): center of gravity of the N(41)-pyrazolyl ring. Symmetry transformations used to generate equivalent atoms: $-x+1$, $-y+1$, $-z+2$ (#), x, $y-1$, z (*).

Single crystals of complex $\mathbf{4}$(18-c-6) were grown from toluene after the addition of excess 18-crown-6 (Figure 5). The three relevant internal bond angles C(21)−B(1)−N(11) = 103.2(1)°, B(1)−N(11)−N(12) = 120.9(1)°, and N(11)−N(12)−Mn(1) = 120.0(1)° of the mono(pyrazol-1-yl)borate side arm are close to the ideal values of 109° for an sp^3-hybridized B atom and 120° for an sp^2-hybridized N atom (torsion angle C(21)−B(1)−N(11)−N(12) = 1.8(2)°). Moreover, the B−C$_5$H$_4$ bond possesses the same length as in the open-chain species ($\mathbf{4}$(18-c-6): 1.626(2) Å, ($\mathbf{3}$THF)$_2$: 1.623(3) Å), and the Mn−pz bond length of 2.026(1) Å in $\mathbf{4}$(18-c-6) is identical to the corresponding value in the pyrazole complex CpMn(CO)$_2$pzH (**8**: Mn(1)−N(11) = 2.024(2) Å; cf. also dicarbonyl[η^5-(8-quinolyl)cyclopentadienyl]-manganese(I): Mn−N = 2.014(1) Å;[37] the Mn−N bonds of several related complexes (C$_5$H$_4$R)Mn(CO)$_2$ with chelating (pyrazol-1-yl)methyl side arms R lie in the range of Mn−N = 2.006(2)−2.066(3) Å[38−40,42]). The B−pz bond is elongated by 0.048 Å in $\mathbf{4}$(18-c-6) (1.606(2) Å) with respect to ($\mathbf{3}$THF)$_2$ (mean value: 1.558(3) Å). It is revealing to compare the average Mn−C and C−O bond lengths of the Mn(I) carbonyl fragments in CymBBr$_2$, ($\mathbf{3}$THF)$_2$, and $\mathbf{4}$(18-c-6) (Mn−C: 1.820(8), 1.796(3), and 1.769(2) Å; C−O: 1.142(9), 1.159(4), and 1.175(2) Å). Along this series, we find a continuous decrease of the Mn−C bond lengths accompanied by an increase of the C−O bond lengths. This trend is in accord with an increasing degree of Mn→CO π back-bonding upon going from a derivative bearing a BBr$_2$ π-acceptor substituent at the cyclopentadienyl

---

(46) Scholz, S.; Green, J. C.; Lerner, H.-W.; Bolte, M.; Wagner, M. *Chem. Commun.* **2002**, 36−37.

(47) Honeyman, G. W.; Kennedy, A. R.; Mulvey, R. E.; Sherrington, D. C. *Organometallics* **2004**, *23*, 1197−1199.

(48) Jones, J. N.; Moore, J. A.; Cowley, A. H.; Macdonald, C. L. B. *Dalton Trans.* **2005**, 3846−3851.

(49) Sänger, I.; Heilmann, J. B.; Bolte, M.; Lerner, H.-W.; Wagner, M. *Chem. Commun.* **2006**, 2027−2029.

(50) Sarazin, Y.; Hughes, D. L.; Kaltsoyannis, N.; Wright, J. A.; Bochmann, M. *J. Am. Chem. Soc.* **2007**, *129*, 881−894.

(51) Sarazin, Y.; Kaltsoyannis, N.; Wright, J. A.; Bochmann, M. *Organometallics* **2007**, *26*, 1811−1815.

(52) Morris, J. J.; Noll, B. C.; Honeyman, G. W.; O'Hara, C. T.; Kennedy, A. R.; Mulvey, R. E.; Henderson, K. W. *Chem.−Eur. J.* **2007**, *13*, 4418−4432.

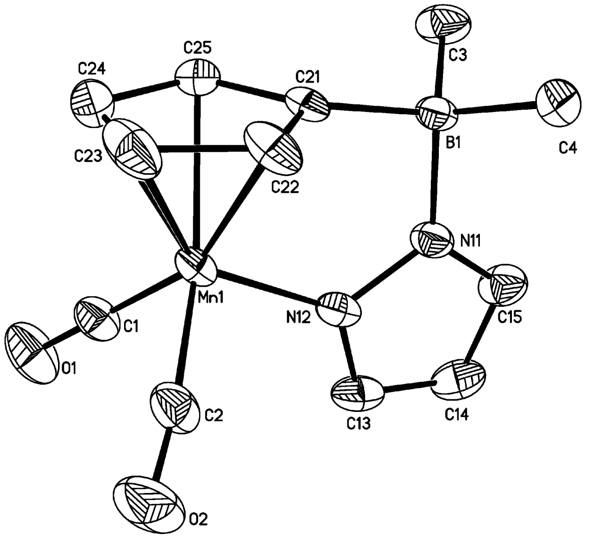

Figure 5. Structure of **4**(18-c-6) in the crystal. Hydrogen atoms and $[K(18\text{-crown-}6)]^+$ ion are omitted for clarity; thermal ellipsoids are drawn at the 50% probability level. Selected bond lengths (Å), angles (deg), torsion angles (deg), and dihedral angles (deg): B(1)−C(3) = 1.636(2), B(1)−C(4) = 1.630(2), B(1)−C(21) = 1.626(2), B(1)−N(11) = 1.606(2), Mn(1)−N(12) = 2.026(1), K(1)−O(1) = 2.684(1); C(21)−B(1)−N(11) = 103.2(1), B(1)−N(11)−N(12) = 120.9(1), N(11)−N(12)−Mn(1) = 120.0(1), COG-(Cp)−C(21)−B(1) = 170.1; C(21)−B(1)−N(11)−N(12) = 1.8(2); $C_5H_5//C_3H_3N_2$ = 83.1. COG(Cp): center of gravity of the cyclopentadienyl ring.

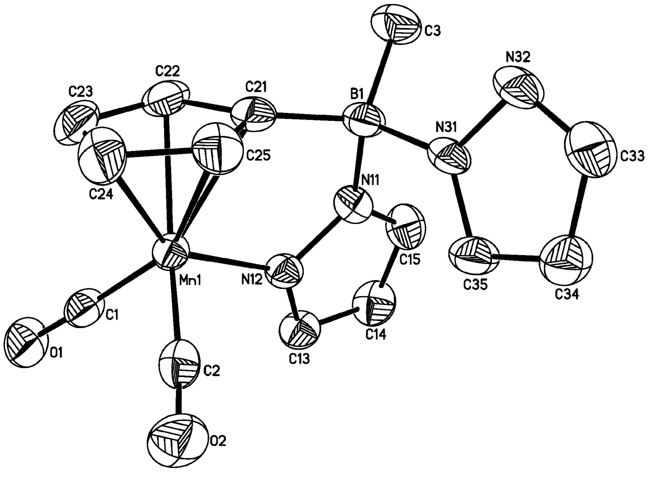

Figure 6. Structure of **5**(18-c-6) in the crystal. Hydrogen atoms and $[K(18\text{-crown-}6)]^+$ ion are omitted for clarity; thermal ellipsoids are drawn at the 50% probability level. Selected bond lengths (Å), angles (deg), torsion angles, and dihedral angles (deg): B(1)−C(3) = 1.602(4), B(1)−C(21) = 1.616(4), B(1)−N(11) = 1.583(3), Mn-(1)−N(12) = 2.030(2), K(1)−O(1) = 2.960(2), K($1^\#$)−N(32) = 2.919(2); C(21)−B(1)−N(11) = 103.1(2), B(1)−N(11)−N(12) = 119.6(2), N(11)−N(12)−Mn(1) = 118.8(2), COG(Cp)−C(21)−B(1) = 168.4; C(21)−B(1)−N(11)−N(12) = −21.7(3); $C_5H_5//C_3H_3N_2$ = 74.0. COG(Cp): center of gravity of the cyclopentadienyl ring. Symmetry transformation used to generate equivalent atoms: $x+1$, $y-1$, z (#).

ring to a species in which one of three electron-withdrawing CO ligands has been replaced by a strong σ donor.

The structural parameters of the core frameworks of **5**(18-c-6) and **6**(18-c-6) (Figures 6, 7) do not deviate significantly from those of **4**(18-c-6), except for the fact that the B(1)−N(11) bonds are somewhat shorter (**5**(18-c-6): 1.583(3) Å, **6**(18-c-6): 1.569(3) Å) and that the torsion angles C(21)−B(1)−N(11)−N(12) are slightly larger (**5**(18-c-6): −21.7(3)°, **6**(18-c-6): 15.1-(3)°) in the bis- and tris(pyrazol-1-yl)borate derivatives. A concluding glimpse at the crystal lattices reveals a bond between the $[K(18\text{-crown-}6)]^+$ cation and the carbonyl oxygen atom O(1) in the case of **4**(18-c-6) (2.684(1) Å), polymer chains with short K(1)−O(1) = 2.960(2) Å and K($1^\#$)−N(32) = 2.919(2) Å contacts in **5**(18-c-6), and a K^+−pyrazolyl bond in **6**(18-c-6) (K(1)−N(32) = 2.872(2) Å).

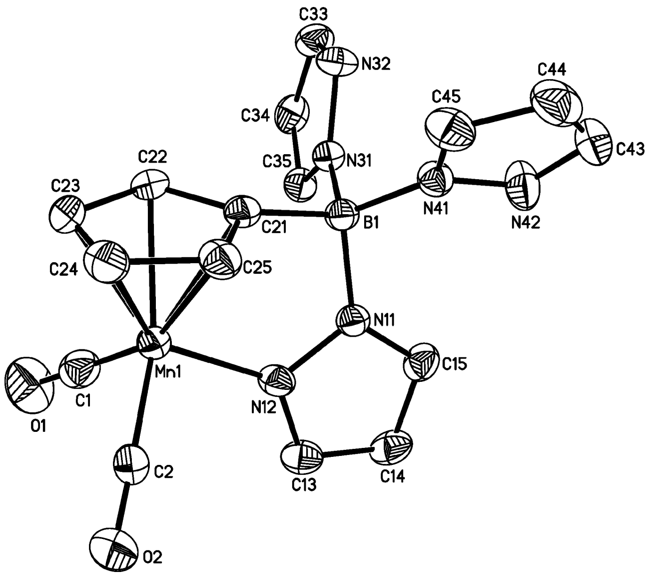

Figure 7. Structure of **6**(18-c-6) in the crystal. Hydrogen atoms and $[K(18\text{-crown-}6)]^+$ ion are omitted for clarity. Thermal ellipsoids are drawn at the 50% probability level. Selected bond lengths (Å), angles (deg), torsion angles, and dihedral angles (deg): B(1)−C(21) = 1.614(3), B(1)−N(11) = 1.569(3), B(1)−N(31) = 1.564(3), B(1)−N(41) = 1.532(3), Mn(1)−N(12) = 2.017(2), K(1)−N(32) = 2.872(2); C(21)−B(1)−N(11) = 106.0(2), B(1)−N(11)−N(12) = 118.2(2), N(11)−N(12)−Mn(1) = 120.1(1), COG(Cp)−C(21)−B(1) = 167.7; C(21)−B(1)−N(11)−N(12) = 15.1(3); $C_5H_5//C_3H_3N_2$ = 83.3. COG(Cp): center of gravity of the cyclopentadienyl ring.

The lithium cymantrenyltris(phenyl)borate **7** crystallizes as a dibutyl ether adduct and forms centrosymmetric dimers in the solid state (($\mathbf{7}OBu_2)_2$; Figure 8). In contrast to (**2**THF$)_2$ and (**3**THF$)_2$, the dimers of ($\mathbf{7}OBu_2)_2$ are held together not by bridging (pyrazol-1-yl)borate ligands but by bridging cymantrenyl fragments. Thus, two of the three carbonyl ligands of each cymantrenyl substituent take part in Li^+ coordination (Li(1)−O(1) = 1.976(9) Å, Li($1^\#$)−O(2) = 2.045(8) Å). In addition to two carbonyl oxygen atoms, each Li^+ ion binds one dibutyl ether ligand and coordinates to the π face of one phenyl substituent (the other two phenyl rings of each borate moiety remain uncomplexed). The Li^+ ion is significantly shifted away from a position above the center of gravity of the six-membered ring toward the carbon atom C(43) (Li(1)−C(43) = 2.482-(10) Å).

The molecular structure of **8** (Figure 9) was determined in order to be able to compare the Mn−N bond lengths in the complexes **4**(18-c-6)−**6**(18-c-6) with the corresponding value in a related unstrained system. Our results show that the Mn(1)−N(11) distance of 2.024(2) Å in **8** is the same as in the other three molecules even though the dihedral angle between the planes of the cyclopentadienyl ring and the pyrazolyl ligand is 30.2° in **8**, but 83.1° in **4**(18-c-6), 74.0° in **5**(18-c-6), and 83.3° in **6**(18-c-6).

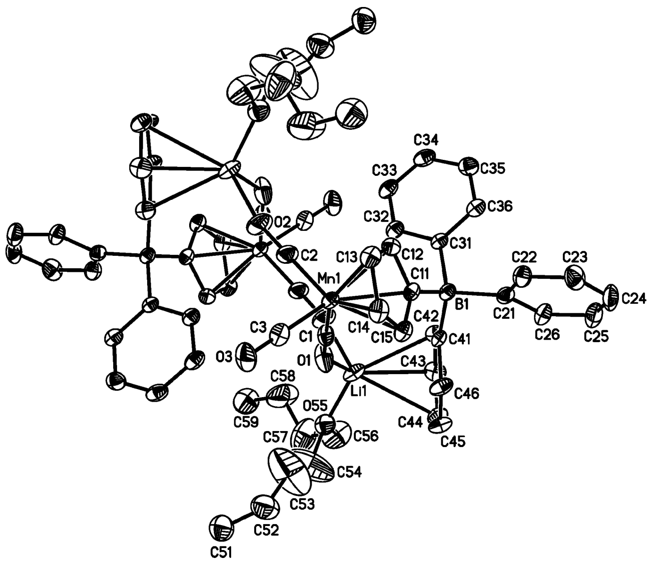

Figure 8. Structure of ($\mathbf{7}OBu_2)_2$ in the crystal. Hydrogen atoms are omittied for clarity; thermal ellipsoids are drawn at the 30% probability level. Selected bond lengths (Å), atom···atom distances (Å), and angles (deg): B(1)−C(11) = 1.659(6), B(1)−C(21) = 1.658(6), B(1)−C(31) = 1.648(6), B(1)−C(41) = 1.650(7), Li(1)−C(42) = 2.578(11), Li(1)−C(43) = 2.482(10), Li(1)−C(44) = 2.732(9), Li(1)−COG(Ph) = 2.450, Li(1)−O(1) = 1.976(9), Li(1)−O($2^{\#}$) = 2.045(8), Li(1)···Li($1^{\#}$) = 7.029; C(21)−B(1)−C(31) = 109.9(4), C(21)−B(1)−C(41) = 107.0(3), C(31)−B(1)−C(41) = 110.9(3). COG(Ph): center of gravity of the C(41)-phenyl ring. Symmetry transformation used to generate equivalent atoms: $-x+1$, $-y+1$, $-z+1$ (#).

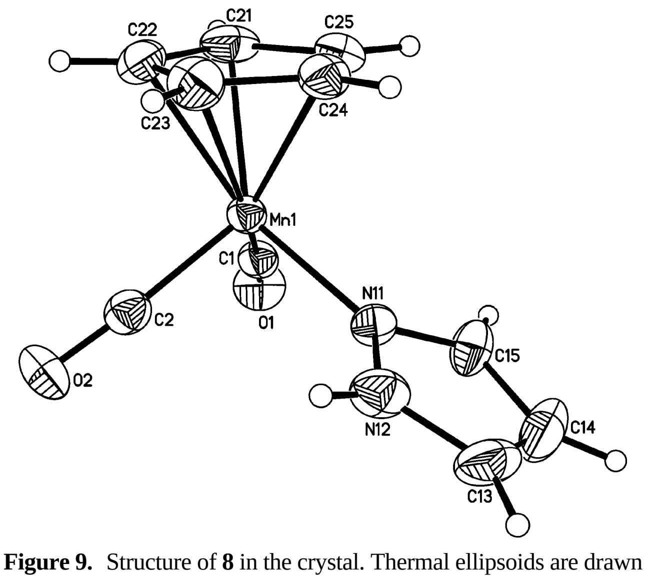

Figure 9. Structure of **8** in the crystal. Thermal ellipsoids are drawn at the 50% probability level. Selected bond lengths (Å), angles (deg), and dihedral angles (deg): Mn(1)−N(11) = 2.024(2), Mn(1)−C(1) = 1.763(3), Mn(1)−C(2) = 1.781(3), C(1)−O(1) = 1.169(4), C(2)−O(2) = 1.174(4); C(1)−Mn(1)−C(2) = 88.2(1), C(1)−Mn(1)−N(11) = 93.8(1), C(2)−Mn(1)−N(11) = 96.7(1); $C_5H_5//C_3H_4N_2$ = 30.2.

Conclusion

The constrained-geometry complexes $K[(OC)_2Mn(C_5H_4\text{-}B(\mu\text{-}pz)(R)R')]$ (**4**−**6**) are readily accessible by photolytic decarbonylation of cymantrenyl-substituted mono-, bis-, and tris(pyrazol-1-yl)borates $K[(OC)_3Mn(C_5H_4\text{-}B(pz)(R)R')]$ (**1**: R = R′ = Me; **2**: R = Me, R′ = pz; **3**: R = R′ = pz; pz = pyrazol-1-yl). X-ray crystal structure analyses of **4**(18-c-6), **5**(18-c-6), and **6**(18-c-6) clearly reveal the respective anionic moieties to be largely unstrained and, consequently, that the cyclopentadienyl/mono(pyrazol-1-yl)borate chelate ligand is well designed to meet the coordination requirements of a $[Mn(CO)_2]^+$ complex fragment. This interpretation is further supported by the ^1H and ^{13}C NMR spectra of **4**−**6** (d_8-THF), which do not give an indication either for dissociation of the chelating pyrazolyl tether or for the formation of a solvent-stabilized open form. In contrast to comparable constrained-geometry species like half-sandwich amido, imido, or alkoxy complexes, the pyrazolyl sidearm is merely a σ donor with less ability to provide additional π-electron density to the metal ion.

The cyclopentadienyl/scorpionate hybrid system opens up interesting perspectives for further development: (i) The steric and/or electronic properties of the ligand scaffold can be modified at will using well-established poly(pyrazol-1-yl)borate synthesis protocols. (ii) (Hetero)bimetallic complexes can be prepared by using the remaining two pyrazolyl substituents of $K[(OC)_2Mn(C_5H_4\text{-}B(\mu\text{-}pz)pz_2)]$ (**6**) for the chelation of a second metal ion.

Moreover, we are currently trying to broaden the scope of our hybrid ligand system by preparing complexes of metal ions other than Mn(I).

Experimental Section

General Remarks. All reactions were carried out under a nitrogen atmosphere using Schlenk tube techniques. Solvents were freshly distilled under argon from Na/benzophenone (toluene, C_6D_6, THF, d_8-THF) and Na/Pb alloy (pentane, hexane) prior to use. NMR: Bruker AM 250, Avance 250, Avance 300, and Avance 400. Chemical shifts are referenced to residual solvent signals (^1H, $^{13}C\{^1H\}$) or external $BF_3{\cdot}Et_2O$ ($^{11}B\{^1H\}$). Abbreviations: s = singlet, d = doublet, vtr = virtual triplet, mult = multiplet, n.r. = multiplet expected in the ^1H NMR spectrum but not resolved, n.o. = signal not observed, br = broad. Bridging pyrazolyl substituents are denoted with an asterisk (pz*). The compounds $CymBBr_2$, $CymBMe_2$, $CymB(NMe_2)_2$,[28] and $H[CymBpz_3]$[23] were synthesized according to published procedures.

Synthesis of CymB(NMe$_2$)Br. To a solution of $CymB(NMe_2)_2$ (0.98 g, 3.25 mmol) in toluene (15 mL) was added dropwise with stirring at rt a solution of $CymBBr_2$ (1.21 g, 3.25 mmol) in toluene (15 mL). The reaction mixture was stirred overnight at rt, and the solvent was removed *in vacuo*. $CymB(NMe_2)Br$ was obtained in the form of yellow crystals. Yield: 2.05 g (93%). IR (toluene, cm^{-1}): $\tilde{\nu}$(CO) 2022 (s), 1935 (s). $^{11}B\{^1H\}$ NMR (96.3 MHz, C_6D_6): δ 33.5 ($h_{1/2}$ = 160 Hz). ^1H NMR (300.0 MHz, C_6D_6): δ 2.31, 2.59 (2 × s, 2 × 3H, NMe_2), 4.11, 4.69 (2 × vtr, 2 × 2H, $^3J_{HH} = {}^4J_{HH}$ = 1.9 Hz, C_5H_4). $^{13}C\{^1H\}$ NMR (75.4 MHz, C_6D_6): δ 40.3, 43.3 (NMe_2), 84.7, 93.0 (C_5H_4), 224.9 (CO), n.o. (CB).

Synthesis of CymB(NMe$_2$)Me. To a solution of $CymB(NMe_2)$-Br (8.78 g, 26.00 mmol) in toluene (70 mL) was added dropwise with stirring at −78 °C a solution of MeMgCl in THF (8.67 mL, 26.00 mmol, 3 mol/L). The reaction mixture was slowly warmed to rt and stirred overnight. After a colorless precipitate had been removed by filtration, the clear filtrate was evaporated *in vacuo*. The resulting yellow oil was stirred overnight with hexane (50 mL). Subsequently, insoluble material was removed by filtration. All volatiles were removed from the filtrate *in vacuo* to give CymB-(NMe_2)Me as a yellow oil. Yield: 4.72 g (67%). IR (toluene, cm^{-1}): $\tilde{\nu}$(CO) 2017 (s), 1921 (s). $^{11}B\{^1H\}$ NMR (96.3 MHz, C_6D_6): δ 39.8 ($h_{1/2}$ = 131 Hz). ^1H NMR (300.0 MHz, C_6D_6): δ 0.44 (s, 3H, CH_3), 2.38, 2.44 (2 × s, 2 × 3H, NMe_2), 4.17, 4.43 (2 × vtr, 2 × 2H, $^3J_{HH} = {}^4J_{HH}$ = 2.0 Hz, C_5H_4). $^{13}C\{^1H\}$ NMR (62.9 MHz, C_6D_6): δ 4.4 (br, CH_3), 40.4, 40.7 (NMe_2), 84.2, 90.8 (C_5H_4), 225.9 (CO), n.o. (CB).

Synthesis of 1. A suspension of Kpz (0.25 g, 2.36 mmol) in THF (15 mL) was added dropwise with stirring at −78 °C to a solution of CymBMe$_2$ (0.58 g, 2.38 mmol) in toluene (40 mL). The reaction mixture was slowly warmed to rt and stirred overnight. After a small amount of colorless precipitate had been removed by filtration, the clear filtrate was evaporated to dryness *in vacuo*. The resulting brown oil was stirred with pentane (15 mL) overnight, whereupon it solidified. After filtration, the insoluble residue was dried *in vacuo* to give a solid foam. Yield of **1**: 0.80 g (97%). IR (KBr, cm^{-1}): $\tilde{\nu}$(CO) 2004 (s), 1910 (s). ^{11}B{^{1}H} NMR (96.3 MHz, d_8-THF): δ −8.7 ($h_{1/2}$ = 100 Hz). ^{1}H NMR (300.0 MHz, d_8-THF): δ 0.00 (s, 6H, CH$_3$), 4.45, 4.46 (2 × n.r., 2 × 2H, C$_5$H$_4$), 5.94 (n.r., 1H, pzH-4), 7.24, 7.46 (2 × n.r., 2 × 1H, pzH-3,5). ^{13}C{^{1}H} NMR (75.4 MHz, d_8-THF): δ 14.0 (CH$_3$), 81.7, 89.4 (C$_5$H$_4$), 102.6 (pzC-4), 132.5, 137.0 (pzC-3,5), 229.2 (CO), n.o. (CB). Anal. Calcd for $C_{13}H_{13}BKMnN_2O_3$ (350.10): C, 44.60; H, 3.74; N, 8.00. Found: C, 43.79; H, 4.11; N, 7.29.

Synthesis of 2. A mixture of Hpz (1.18 g, 17.33 mmol) and Kpz (1.84 g, 17.33 mmol) in THF (25 mL) was added dropwise with stirring at −78 °C to a solution of CymB(NMe$_2$)Me (4.72 g, 17.29 mmol) in toluene (50 mL). The reaction mixture was slowly warmed to rt and stirred overnight. After a small amount of colorless precipitate had been removed by filtration, the clear filtrate was evaporated to dryness *in vacuo*. The resulting orange oil was stirred with pentane (25 mL) overnight, whereupon it solidified. The colorless microcrystalline solid was collected on a frit and dried *in vacuo*. Yield of **2**·THF: 6.96 g (85%). The solid material contained light yellow single crystals of (**2**THF)$_2$, which were suitable for X-ray crystallography. IR (KBr, cm^{-1}): $\tilde{\nu}$(CO) 2009 (s), 1920 (s). ^{11}B{^{1}H} NMR (128.4 MHz, d_8-THF): δ −1.1 ($h_{1/2}$ = 92 Hz). ^{1}H NMR (400.1 MHz, d_8-THF): δ 0.55 (s, 3H, CH$_3$), 4.55, 4.77 (2 × vtr, 2 × 2H, $^3J_{HH}$ = $^4J_{HH}$ = 1.8 Hz, C$_5$H$_4$), 6.00 (vtr, 2H, $^3J_{HH}$ = 1.8 Hz, pzH-4), 7.30, 7.54 (n.r., d, 2 × 2H, $^3J_{HH}$ = 2.0 Hz, pzH-3,5). ^{13}C{^{1}H} NMR (100.6 MHz, d_8-THF): δ 81.6, 92.3 (C$_5$H$_4$), 103.2 (pzC-4), 133.1, 138.8 (pzC-3,5), n.o. (2 × CB, CO). Anal. Calcd for $C_{15}H_{13}BKMnN_4O_3$ (402.14) × OC_4H_8 (72.11): C, 48.12; H, 4.46; N, 11.81. Found: C, 48.00; H, 4.57; N, 11.89.

Synthesis of 3. A suspension of KO*t*Bu (0.26 g, 2.32 mmol) in THF (20 mL) was added dropwise with stirring at 0 °C to a solution of H[CymBpz$_3$][23] (0.95 g, 2.28 mmol) in THF (10 mL). The reaction mixture was slowly warmed to rt and stirred overnight and the resulting yellow solution evaporated to dryness *in vacuo*. The remaining yellow oil was stirred with pentane (15 mL) overnight, whereupon it solidified. The colorless microcrystalline solid was collected on a frit and dried *in vacuo*. Yield of **3**·THF: 0.93 g (78%). Yellow single crystals of (**3**THF)$_2$ formed upon storing a solution of **3** in THF/pentane (1:1) at −35 °C. IR (KBr, cm^{-1}): $\tilde{\nu}$(CO) 2006 (s), 1921 (s). UV/vis (THF, $c = 7 \times 10^{-4}$ mol·L^{-1}, nm): λ_{max} = 330 (ϵ = 1110 L·mol^{-1}·cm^{-1}). ^{11}B{^{1}H} NMR (128.4 MHz, d_8-THF): δ 0.1 ($h_{1/2}$ = 80 Hz). ^{1}H NMR (400.1 MHz, d_8-THF): δ 4.67, 4.82 (2 × vtr, 2 × 2H, $^3J_{HH}$ = $^4J_{HH}$ = 1.7 Hz, C$_5$H$_4$), 6.08 (vtr, 3H, $^3J_{HH}$ = 1.8 Hz, pzH-4), 7.32, 7.39 (d, $^3J_{HH}$ = 2.0 Hz, n.r., 2 × 3H, pzH-3,5). ^{13}C{^{1}H} NMR (100.6 MHz, d_8-THF): δ 82.9, 91.6 (C$_5$H$_4$), 104.0 (pzC-4), 135.1, 139.7 (pzC-3,5), 227.2 (CO), n.o. (CB). Anal. Calcd for $C_{17}H_{13}BKMnN_6O_3$ (454.17) × OC_4H_8 (72.11): C, 47.93; H, 4.02; N, 15.97. Found: C, 48.09; H, 4.05; N, 16.25.

Synthesis of 4. A solution of **1** (0.06 g, 0.17 mmol) in THF (15 mL) was placed in a borosilicate glass vessel and irradiated with a high-pressure mercury lamp (λ_{max} = 510 nm). After 6 h, the transformation of **1** to **4** was quantitative (NMR spectroscopical control). All volatiles were removed *in vacuo*, and the remaining red-brown residue was washed with pentane (20 mL), isolated by filtration, and dried *in vacuo*. Red X-ray quality crystals of **4**(18-c-6) formed at rt from a solution of **4** in toluene to which excess 18-crown-6 had been added. IR (KBr, cm^{-1}): $\tilde{\nu}$(CO) 1891 (s), 1817 (s). ^{11}B{^{1}H} NMR (128.4 MHz, d_8-THF): δ −8.1 ($h_{1/2}$ = 75 Hz). ^{1}H NMR (250.1 MHz, d_8-THF): δ −0.17 (s, 6H, CH$_3$), 3.53 (vtr, 2H, $^3J_{HH}$ = $^4J_{HH}$ = 1.7 Hz, C$_5$H$_4$), 3.61 (s, 24H, 18-c-6), 4.93 (vtr, 2H, $^3J_{HH}$ = $^4J_{HH}$ = 1.7 Hz, C$_5$H$_4$), 5.72 (vtr, 1H, $^3J_{HH}$ = 2.0 Hz, pz*H-4), 6.78, 6.94 (n.r., d, $^3J_{HH}$ = 2.0 Hz, 2 × 1H, pz*H-3,5). ^{13}C{^{1}H} NMR (100.6 MHz, d_8-THF): δ 71.2 (18-c-6), 78.1, 84.1 (C$_5$H$_4$), 104.1 (pz*C-4), 131.4, 142.6 (pz*C-3,5), n.o. (CB, CO). Anal. Calcd for $C_{12}H_{13}BKMnN_2O_2$ (322.09) × $C_{12}H_{24}O_6$ (264.32): C, 49.16; H, 6.36; N, 4.78. Found: C, 48.99; H, 6.40; N, 4.70.

Synthesis of 5. A solution of **2**·THF (0.26 g, 0.55 mmol) in THF (15 mL) was placed in a borosilicate glass vessel and irradiated with a high-pressure mercury lamp (λ_{max} = 510 nm). After 6 h, the transformation of **2** to **5** was quantitative (NMR spectroscopical control). All volatiles were removed *in vacuo*, and the remaining orange residue was washed with pentane (20 mL), isolated by filtration, and dried *in vacuo*. Orange X-ray quality crystals of **5**(18-c-6) formed at rt from a solution of **5** in toluene to which excess 18-crown-6 had been added. IR (KBr, cm^{-1}): $\tilde{\nu}$(CO) 1890 (s), 1813 (s). ^{11}B{^{1}H} NMR (128.4 MHz, d_8-THF): δ −2.0 ($h_{1/2}$ = 100 Hz). ^{1}H NMR (400.1 MHz, d_8-THF): δ 0.32 (s, 3H, CH$_3$), 3.65 (s, 24H, 18-c-6), 3.45, 3.65, 4.71, 4.97 (4 × n.r., 4 × 1H, C$_5$H$_4$), 5.84, 5.89 (2 × n.r., 2 × 1H, pz*H-4, pzH-4), 6.95, 6.98, 7.23, 7.31 (4 × n.r., 4 × 1H, pz*H-3,5, pzH-3,5). ^{13}C{^{1}H} NMR (100.6 MHz, d_8-THF): δ 70.9 (18-c-6), 77.4, 79.0, 83.9, 86.1 (C$_5$H$_4$), 101.9, 105.1 (pz*C-4, pzC-4), 131.5, 133.6, 137.9, 144.2 (pz*C-3,5, pzC-3,5), n.o. (2 × CB, CO). Anal. Calcd for $C_{14}H_{13}BKMnN_4O_2$ (374.13) × $C_{12}H_{24}O_6$ (264.32) × C_7H_8 (92.14): C, 54.25; H, 6.21; N, 7.67. Found: C, 54.71; H, 6.24; N, 7.57.

Synthesis of 6. A solution of **3**·THF (0.11 g, 0.21 mmol) in THF (15 mL) was placed in a borosilicate glass vessel and irradiated with a high-pressure mercury lamp (λ_{max} = 510 nm). After 6 h, the transformation of **3** to **6** was quantitative (NMR spectroscopical control). All volatiles were removed *in vacuo*, and the remaining orange residue was washed with pentane (20 mL), isolated by filtration, and dried *in vacuo*. Orange X-ray quality crystals of **6**(18-c-6) formed at rt from a solution of **6** in toluene/THF to which excess 18-crown-6 had been added. IR (KBr, cm^{-1}): $\tilde{\nu}$(CO) 1902 (s), 1824 (s). UV/vis (THF, $c = 7 \times 10^{-4}$ mol·L^{-1}, nm): λ_{max} = 280 (ϵ = 2990 L·mol^{-1}·cm^{-1}), 312 (ϵ = 2770 L·mol^{-1}·cm^{-1}), ∼400 (v br, onset at ∼550, ϵ(400 nm) = 390 L·mol^{-1}·cm^{-1}). ^{11}B{^{1}H} NMR (96.3 MHz, d_8-THF): δ −0.1 ($h_{1/2}$ = 70 Hz). ^{1}H NMR (300.0 MHz, d_8-THF): δ 3.57 (s, 24H, 18-c-6), 3.57, 5.04, (1 × n.r., 1 × vtr, 2 × 2H, $^3J_{HH}$ = $^4J_{HH}$ = 1.9 Hz, C$_5$H$_4$), 5.88 (mult, 1H, pz*H-4), 5.96 (mult, 2H, pzH-4), 7.01 (n.r., 1H, pz*H-3 or 5), 7.17, 7.36 (2 × mult, 2 × 2H, pzH-3,5), 7.64 (d, 1H, $^3J_{HH}$ = 2.1 Hz, pz*H-5 or 3). ^{13}C{^{1}H} NMR (75.4 MHz, d_8-THF): δ 71.4 (18-c-6), 79.0, 86.9 (C$_5$H$_4$), 103.0 (pzC-4), 106.0 (pz*C-4), 133.6 (pzC-3 or 5), 136.8 (pz*C-3 or 5), 139.7 (pzC-5 or 3), 145.9 (pz*C-5 or 3), n.o. (CB, CO). Anal. Calcd for $C_{16}H_{13}BKMnN_6O_2$ (426.16) × $C_{12}H_{24}O_6$ (264.32): C, 48.71; H, 5.40; N, 12.17. Found: C, 48.70; H, 5.47; N, 12.20.

Synthesis of 7. To a solution of CymBBr$_2$ (2.60 g, 6.96 mmol) in toluene (25 mL) was added dropwise with stirring at −78 °C PhLi in Bu$_2$O (10.50 mL, 21.00 mmol, 2 mol/L). The reaction mixture was slowly warmed to rt and stirred overnight. The reaction mixture was filtered, and the filtrate was evaporated to dryness *in vacuo*. The resulting brown oil was contaminated with substantial amounts of Li[BPh$_4$], which could not be removed completely. A few single crystals of (**7**OBu$_2$)$_2$ formed upon storing a solution of Li[CymBPh$_3$] in toluene/hexane (1:1) at −35 °C. IR (KBr, cm^{-1}): $\tilde{\nu}$(CO) 2000 (s), 1911 (s). ^{11}B{^{1}H} NMR (128.4 MHz, C$_6$D$_6$): δ −9.5 ($h_{1/2}$ = 14 Hz). ^{1}H NMR (400.1 MHz, C$_6$D$_6$): δ 4.44, 4.60 (2 × n.r., 2 × 2H, C$_5$H$_4$), 7.02 (vtr, 3H, $^3J_{HH}$ = 6.7 Hz, *p*-Ph), 7.22 (vtr, 6H, $^3J_{HH}$ = 6.6 Hz, *m*-Ph), 7.61 (d, 6H, $^3J_{HH}$ = 5.4 Hz, *o*-Ph). ^{13}C{^{1}H} NMR (62.9 MHz, C$_6$D$_6$): δ 85.3, 90.3 (C$_5$H$_4$), 123.9, 127.1, 136.0 (Ph), 230.5 (CO), n.o. (2 × CB). A decent elemental analysis of **7** was not obtained due to contamination of the sample with Li[BPh_4].

Synthesis of 8. To a solution of CymH (3.45 g, 16.9 mmol) in diethyl ether (200 mL) was added Hpz (1.15 g, 16.9 mmol). The reaction mixture was irradiated using a UV lamp (TQ 150, λ_{max} = 510 nm) for 50 h, whereupon the yellow solution turned orange. The solvent was removed *in vacuo* and the resulting orange oil stored at −35 °C. After 3 weeks, a few orange single crystals of **8** had formed, which were suitable for X-ray crystallography. IR (KBr, cm^{-1}): $\tilde{\nu}$(CO) 1913 (s), 1837 (s). ^1H NMR (250.1 MHz, Et_2O/C_6D_6): δ 4.22 (s, 5H, C_5H_5), 5.94 (br, 1H, pzH-4), 7.29 (br, 2H, pzH-3,5), 11.46 (br, 1H, NH).

X-ray Crystal Structure Analysis of CymBBr$_2$, (2THF)$_2$, (3THF)$_2$, 4(18-c-6), 5(18-c-6), 6(18-c-6), (7OBu$_2$)$_2$, and 8. All single crystals were analyzed with a STOE IPDS II two-circle diffractometer with graphite-monochromated Mo Kα radiation. Empirical absorption corrections were performed using the MULABS[53] option in PLATON.[54] The structures were solved by direct methods using the program SHELXS[55] and refined against F^2 with full-matrix least-squares techniques using the program SHELXL-97.[56] The coordinated THF molecules of (**3**THF)$_2$ and (**2**THF)$_2$ are disordered over two positions (occupancy factors 0.56(2) and 0.44(2) in both cases). **5**(18-c-6): The asymmetric unit contains one toluene molecule, which is not disordered. CCDC reference numbers: 644558 (CymBBr$_2$), 644559 ((**2**THF)$_2$), 644560 ((**3**THF)$_2$), 644561 (**4**(18-c-6)), 644562 (**5**(18-c-6)), 644563 (**6**(18-c-6)), 644564 ((**7**OBu$_2$)$_2$), and 644565 (**8**).

Acknowledgment. M.W. is grateful to the “Deutsche Forschungsgemeinschaft” (DFG) and the “Fonds der Chemischen Industrie” (FCI) for financial support.

Supporting Information Available: Crystallographic data of CymBBr$_2$, (**2**THF)$_2$, (**3**THF)$_2$, **4**(18-c-6), **5**(18-c-6), **6**(18-c-6), (**7**OBu$_2$)$_2$, and **8** in CIF format. This material is available free of charge via the Internet at http://pubs.acs.org.

OM700450J

---

(53) Blessing, R. H. *Acta Crystallogr. Sect. A* **1995**, *51*, 33−38.

(54) Spek, A. L. *Acta Crystallogr. Sect. A* **1990**, *46*, C34.

(55) Sheldrick, G. M. *Acta Crystallogr. Sect. A* **1990**, *46*, 467−473.

(56) Sheldrick, G. M. *SHELXL-97*, A Program for the Refinement of Crystal Structures; Universität Göttingen, 1997.